Differences in Human Meibum Lipid Composition with Meibomian Gland Dysfunction Using NMR and Principal Component Analysis

Douglas Borchman,[1] *Gary N. Foulks,*[2] *Marta C. Yappert,*[3] *and Sarah E. Milliner*[3]

Purpose. Nuclear magnetic resonance (NMR) spectroscopy has been used to quantify lipid wax, cholesterol ester terpenoid and glyceride composition, saturation, oxidation, and CH_2 and CH_3 moiety distribution. This tool was used to measure changes in human meibum composition with meibomian gland dysfunction (MGD).

Methods. ^{1}H-NMR spectra of meibum from 39 donors with meibomian gland dysfunction (Md) were compared to meibum from 33 normal donors (Mn).

Results. Principal component analysis (PCA) was applied to the CH_2/CH_3 regions of a set of training NMR spectra of human meibum. PCA discriminated between Mn and Md with an accuracy of 86%. There was a bias toward more accurately predicting normal samples (92%) compared with predicting MGD samples (78%). When the NMR spectra of Md were compared with those of Mn, three statistically significant decreases were observed in the relative amounts of CH_3 moieties at 1.26 ppm, the products of lipid oxidation above 7 ppm, and the ═CH moieties at 5.2 ppm associated with terpenoids.

Conclusions. Loss of the terpenoids could be deleterious to meibum since they exhibit a plethora of mostly positive biological functions and could account for the lower level of cholesterol esters observed in Md compared with Mn. All three changes could account for the higher degree of lipid order of Md compared with age-matched Mn. In addition to the power of NMR spectroscopy to detect differences in the composition of meibum, it is promising that NMR can be used as a diagnostic tool. (*Invest Ophthalmol Vis Sci.* 2012;53:337–347) DOI: 10.1167/iovs.11-8551

The correlation between dry eye and an abnormal lipid layer of the tear film has been made by use of interference microscopy[1–5] and other techniques, all reviewed in 2004.[6] Most of the tear lipids are produced by the meibomian gland, and when the gland is dysfunctional, dry-eye conditions ensue.[7,8] When the meibomian gland in patients with dry eye is expressed, the lipid layer thickness increases, as does tear stability.[9,10] The correlation between the lipid layer and dry eye conditions has also been associated with contact lens wear[11,12] and exposure to substances such as solvent vapors, which cause disruption of the lipid layer.[13] Relationships between meibomian gland dysfunction (MGD) and dry eye symptoms have been reviewed.[14–18]

A lipidomics approach to measuring meibum lipid has been reviewed[19] and has been very successful in identifying and discovering unique lipids. A problem with this approach is that complete quantification is complicated by the great number (thousands) of species present in human meibum.[20] Because each lipid class has a different ionization efficiency, standards are needed for the quantification of each of them. The lipid composition of human meibum varies greatly from study to study.[19] This variation has been attributed to the different analytical methodologies employed and the inherent variability of biological samples.[19] Indeed, the lipid composition ranges from study to study are for wax esters (8% to 39%), for cholesterol esters (8% to 39%), for glycerides (0% to 5%), for phospholipids (0% to 16%), and for hydrocarbons (1% to 38%).[19]

Spectroscopic studies have identified changes that occur with MGD that could be important to the function of the tear film. Infrared spectral studies along with the use of principal component analysis (PCA) enable the quantification of the variance among the lipid spectra which identified and quantified the protein (another biomarker of instability) associated with human meibum.[21,22] The spectra were used to discriminate between meibum from normal donors (Mn) and meibum from donors with MGD (Md) with an accuracy of 93%.[22] More importantly, it shows that certain spectral regions (eigenvectors) contain compositional and structural information about the changes that occur with the principal component (or variable). The spectral features, which in this case is MGD, of the major eigenvector provided three biomarkers showing that meibum from donors with MGD (Md) contains more protein and relatively less methyl groups (CH_3) and *cis* double bonds (*cis*═CH) compared to meibum from donors with normal meibomian glands. The amount of protein was confirmed from relative infrared band intensities.[22]

Age-related changes in human meibum have also been observed using spectroscopic analysis. Infrared and nuclear magnetic resonance (NMR) and Raman spectroscopies were used to show that meibum from children has fewer double bonds,[21,23] cholesterol esters,[21,24] and protein[22] and more carotenoids,[23,25] and CH_2 groups[21,23] than older normal adults. It has yet to be determined whether these changes are associated with functional changes, such as the rate of evaporation, tear breakup time and meibum spreading.

From the Departments of [1]Ophthalmology and Visual Sciences and [3]Chemistry, University of Louisville, Louisville, Kentucky; and the [2]Department of Surgery, Robley Rex Veterans Affairs Medical Center, Louisville, Kentucky.

Supported by National Institutes of Health Grant EY017094-01 (GNF), Kentucky Lions Eye Foundation, and an unrestricted grant from Research to Prevent Blindness, Inc. Much of this material is the result of work supported with resources and use of the facilities at the Louisville Veterans Affairs Medical Center, Louisville, Kentucky. GNF is a member of the part-time staff of the Surgical Service, Department of Veteran Affairs Medical Center, Louisville, Kentucky.

Submitted for publication September 7, 2011; revised November 10, 2011; accepted November 15, 2011.

Disclosure: **D. Borchman**, None; **G.N. Foulks**, None; **M.C. Yappert**, None; **S.E. Milliner**, None

Corresponding author: Douglas Borchman, Kentucky Lions Eye Center, 301 E. Muhammad Ali Boulevard, Louisville, KY 40202; borchman@louisville.edu.

TABLE 1. Meibum Donor Grouping and Characteristics

	Average Age (y)	Age Range (y)	Male (%)	Race (%)	Sample (*n*)
Infant	1.1	<1–2	86	C 57, B 14, H 14, U 14	7
Child	7.6	3–12	57	C 71, U 29	7
Adolescent	20	13–21	86	C 86, U 14	7
Adult	54	32–83	82, U9	C 54, B 9, A 9, U 28	11
MGD	67	29–87	72, U3	C7 7, B 13, H 3, U 7	39

C, Caucasian; B, Black; H, Hispanic; U, unknown.

Two other groups have documented changes in meibum composition that may contribute and be diagnostic of dry eye symptoms. The level of wax and cholesterol ester saturation changed in meibum from donors with meibomian keratoconjunctivitis depending on whether the comparison was made with Mn from a population containing cholesterol esters or not.[26] Triglycerides in Md were more saturated compared to those in Mn,[27] and Md had a lower percentage of monounsaturated (oleic acid).[28] Another group has shown that Md contains a lower percentage of saturation and a higher percentage of branched acyl chains.[29] Md also contains higher levels of phosphatidylcholine[30] and phospholipid unsaturation[31] and lower levels of phosphatidylethanolamine and sphingomyelin[32] compared with Mn. There is still controversy about the actual composition of meibum, especially regarding the polar lipids. Discrepancies may depend on the analytical methods, the sample collection techniques, and contamination.[32–36]

Infrared spectroscopic studies show that in MGD, both the lipid order and corresponding phase transition temperature increase, indicating a stiffer lipid arrangement.[37,38] Stiffer meibum lipid could impede the flow of meibum, resulting in less lipid on the lid margin, which leads to a higher rate of tear evaporation. Furthermore, stiffer meibum lipids are unlikely to spread on the surface of the tear film.[1] We hypothesize that the elevated protein content associated with Md causes meibum to be more ordered and, on visual inspection, to appear to be more viscous.[22]

Infrared and Raman spectroscopy have been applied to study meibum hydrocarbon chain conformation and have provided limited information regarding meibum composition.[1,21,22,25,37–42] These techniques may be applicable to high-throughput screening, and FTIR has recently been used as a diagnostic tool.[22] The advantage of spectroscopic techniques is that the sample is not destroyed in the process of analysis, and the same sample can be analyzed later by other techniques including mass spectrometry. NMR analysis has been useful in the identification and characterization of new lipids in the human lens[43–48] and in quantifying waxes and the primary structure and composition of cholesterol esters and triglycerides, which are major components of human meibum.[49–59] In this study, we used NMR spectroscopy to quantify CH_3 and CH_2, ═CH, which are moieties and products of lipid oxidation in human meibum with MGD.

MATERIALS AND METHODS

The following Materials and Methods section is almost identical with that in our prior publications.[23,24]

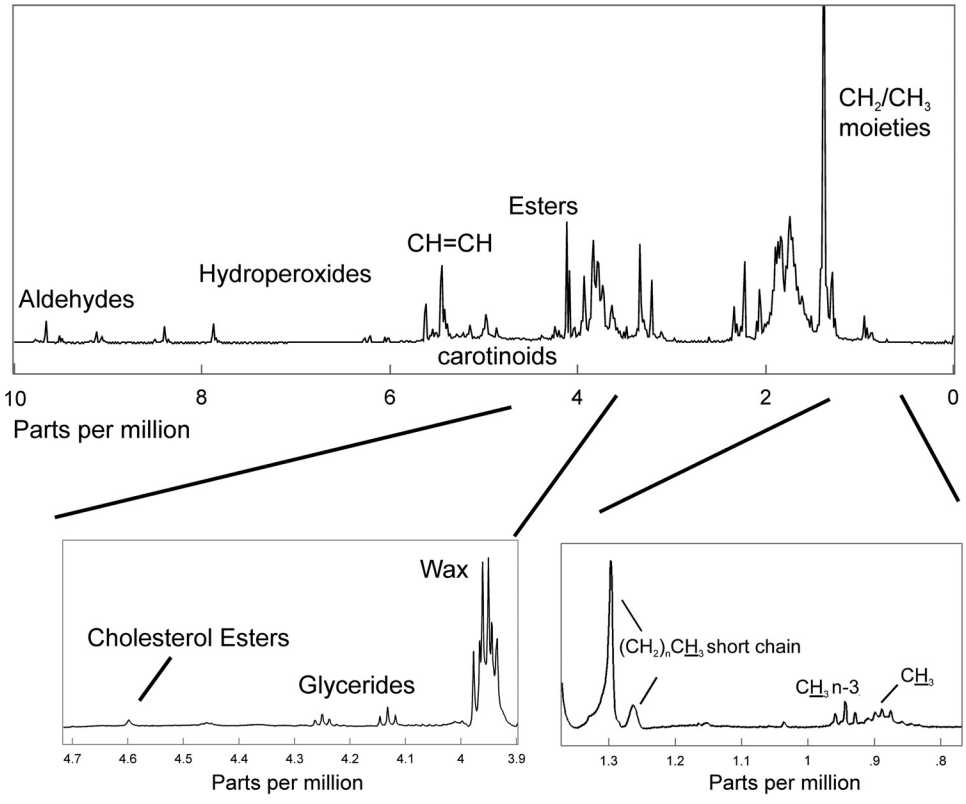

FIGURE 1. The average ^{1}H NMR spectrum of human meibum from donors with MGD. The ^{1}H NMR spectra of human meibum may be divided into five regions: The CH_2 and CH_3 region from 0 to 1.4 ppm, the CH and deshielded CH_2 region from 1.4 to 3.9 ppm, the ester region from 3.9 to 4.7, the C═C region from 4.7 to 7 ppm, and the oxidative products region above 7 ppm. The *insets* at the *bottom* are presented to show more detail.

TABLE 2. Eigenvector Scores

Eigenvector	Normal Group (Mn)	MGD Group (Md)
1	−0.2 ± 0.5	0.3 ± 0.5
2	−0.1 ± 0.4	0.1 ± 0.4
3	−0.1 ± 0.3	0.1 ± 0.2
4	−0.06 ± 0.2	0.1 ± 0.2
5	−0.03 ± 0.1	0.04 ± 0.1
6	−0.02 ± 0.1	0.02 ± 0.1
7	−0.2 ± 0.1	0.02 ± 0.09

Data are the average eigenvector scores ± SD.

Materials

Cyclohexane-d_{12}, tetrahydrofuran (THF) and methanol (MeOH) were obtained from Sigma-Aldrich (St. Louis, MO).

Clinical Diagnosis

Subjects were recruited from the Kentucky Lion's Eye Center and the Robley Rex Veterans Affairs Medical Center in Louisville, KY. Normal status was assigned when the subject's meibomian gland orifices showed no evidence of keratinization or plugging with turbid or thickened secretions and no dilated blood vessels were observed on the eyelid margin.

The diagnosis of MGD was made according to the criteria of Foulks and Bron.[60] Plugging of the meibomian glands of at least 5 of 10 orifices in the central portion of the upper eyelid was required for diagnosis of MGD. The secretion expressed by the meibomian gland had to be turbid, turbid with clumps, or pastelike. Both, inflammation of the eyelid margin, as evidenced by swelling of the eyelid margin, and 2+ vascular injection of the posterior lid margin, were necessary for diagnosis. The presence of telangiectasia of the posterior eyelid margin was confirmatory of chronic disease but not required for entry. Tear film stability was determined by instillation of sodium fluorescein into the tear film. Tear breakup time was <5 seconds for all Md subjects sampled.

Collection and Processing of Human Meibum

Written informed consent was obtained from all donors. Protocols and procedures were reviewed by the institutional review boards of the University of Louisville and Robley Rex Veterans Affairs. All procedures were in accord with the Declaration of Helsinki. The meibomian gland was expressed by compressing the eyelid between cotton-tipped applicators, with strict attention to avoiding touching the eyelid margin during expression. All four eyelids were expressed, and approximately 1 mg of meibum was collected per individual for direct spectroscopic study. The expressate was collected with a platinum spatula and immediately spread onto the AgCl window and into 0.5 mL of THF/MeOH, 3:1 vol:vol, in a 9-mm microvial with a Teflon cap (Microliter Analytical Supplies., Suwanee, GA). All samples were frozen under argon gas until analysis. Analyses were performed within 3 weeks of collection of the sample. Storage of the sample on AgCl windows for more than 2 months under argon did not affect the sample.[25] Before NMR analysis, the THF/MeOH in the microvial containing meibum lipid (ML) rinsed from the spatula was evaporated with a stream of argon gas.

After infrared analysis and solvent evaporation, the ML was removed from the AgCl window by using a series of solvents with different hydrophobicities to ensure that all lipid classes were extracted from the AgCl window. First, the AgCl window was placed with the ML side down, into a 15-mL glass scintillation vial containing 1 mL of hexane and purged with argon gas. A glass vial, rather than a plastic one, was used in all protocols to avoid plasticizer contamination. The vial was sonicated in an ultrasonic bath (model 1510; Branson Ultrasonics, Danbury, CT) for 10 minutes. The hexane was decanted into the microvial containing the ML rinsed from the spatula. The hexane was evaporated under a stream of nitrogen gas. Methanol (1.5 mL) was then added to the scintillation vial containing the AgCl window and purged with argon gas. The vial was sonicated in an ultrasonic bath (Branson Ultrasonics) for 10 minutes. The methanol was decanted into the microvial containing the ML rinsed from the spatula and was evaporated under a stream of nitrogen gas. THF/MeOH (1.5 mL) was added to the scintillation vial containing the AgCl window and purged with argon gas. The vial was sonicated in an ultrasonic bath (Branson Ultrasonics) for 10 minutes. The microvial containing

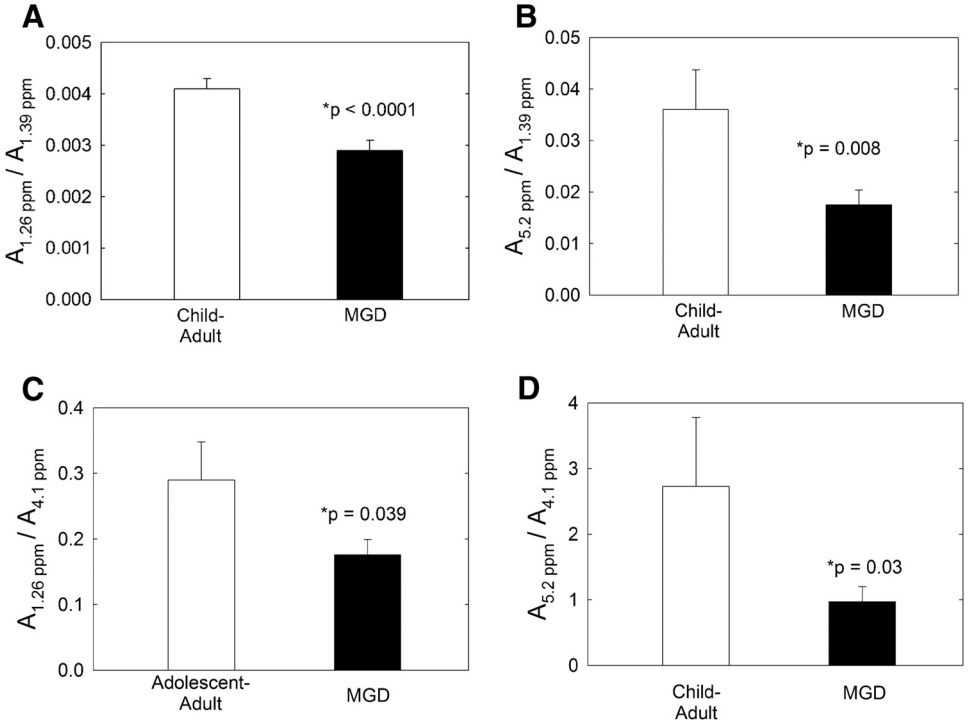

FIGURE 2. Relative area ratios used to compare Mn with Md. The assignment for the proton resonance at 1.26 ppm is uncertain and has been assigned to methylene protons associated with short-chain esters. The area of this resonance was divided by the area of the CH_2 resonance in (**A**) and the area of the wax ester resonance in (**C**). The resonance at 5.2 ppm has been assigned to terpenoid protons in the ═CH— moiety. The area of this resonance was divided by the area of the CH_2 resonance in (**B**) and the area of the wax ester resonance in (**D**).

the extracted meibum lipid was lyophilized for 12 hours to remove trace amounts of organic solvents. Finally, deuterated cyclohexane (0.5 mL) was added to the sample and sonicated (Branson Ultrasonics) for 10 minutes in a bath sonicator. The solution was transferred to glass NMR tubes (Sigma-Aldrich), and the NMR spectra were collected.

NMR Spectral Measurement

Spectral data were acquired (Inova-500 spectrometer; Varian, Lexington, MA). The following parameters were used: 800 scans were acquired with a spectral width of 15 ppm, 60° pulse, 4-K data points, 1.0-second delay time, and 2.049-second acquisition time at 25°C. A computer running commercial software (GRAMS 386; Galactic Industries Corp., Salem, NH) was used for phasing and integrating.

PCA was used to detect subtle differences in the spectral data and to assess whether or not spectra of meibum from normal donors (Mn) differ from those of donors with MGD (Md; analysis performed with GRAMS/386 software; Galactic Industries). For each spectrum, two constituents were used: age and MGD/normal score. The training set was set up by assigning Mn spectra an MGD/normal score of 0 and Md spectra an MGD/normal score of 100.

Statistics

Data are presented as the average ± the standard error of the mean (SEM). Statistical significance was determined using Student's *t*-test or the correlation coefficient from the linear regression best fit. $P < 0.05$ was considered statistically significant.

Results

NMR spectra of Md from 39 donors were compared with Mn spectra from 33 normal donors. The spectra were grouped by age and MGD according to Table 1.

An average of the ^{1}H NMR spectra of human meibum is shown in Figure 1. The ^{1}H NMR spectra of human meibum may be divided into five regions: the CH_2 and CH_3 region from 0 to 1.4 ppm, the CH and deshielded CH_2 region from 1.4 to 3.9 ppm, the ester region from 3.9 to 4.7, the C═C region from 4.7 to 7 ppm, and the oxidative products region above 7 ppm. Tentative band assignments were made from an ^{1}H and ^{13}C NMR study of waxes and triacylglycerols, oils, and waxes[49–59] (Table 2).

The CH_2 and CH_3 Region

The CH_2 and CH_3 ^{1}H NMR resonance region of an average NMR spectrum of human meibum can be seen at the bottom of Figure 1. Five major proton moieties were resolved in the NMR spectra of human meibum (Fig. 1, bottom right). The most intense resonance corresponded to the —$(CH_2)_n$— protons at 1.39 ppm (Fig. 1, bottom right). The resonances near 0.89 ppm were assigned to C**H**$_3$ protons, excluding methylene moieties near omega 3 double bonds (Fig. 1, bottom right). A triplet centered near 0.94 ppm was assigned to methylene moieties near omega 3 double bonds (Fig. 1, bottom right). A less intense proton resonance was observed near 1.03 ppm (Fig. 1) that was assigned tentatively to —CH_2OHC**H**$_2$ C**H**$_3$ and —CH_2—C**H**—$(CH_3)_2$, isobranched protons (Table 2). The assignments for the proton resonances near 1.29 and 1.26 ppm are less certain and have been assigned tentatively to methylene protons associated with short-chain esters (Fig. 1; Table 2), as the proximity of the ester linkage would lead to greater deshielding. Two proton resonances near 0.72 and 0.09 ppm appear in all the NMR spectra of human meibum and are relatively less intense, only a thousandth of the intensity of the 1.39 CH_2 resonance (Table 2, resonance not shown). No proton assignments were made for these resonances.

In comparing the CH_2/CH_3 regions of Mn with Md, only the area of the 1.26 ppm was significantly lower ($P < 0.05$) for Md compared with Mn from children and adults (Figs. 2A, 2C). The relative areas of all the other resonances in the region were similar ($P > 0.05$; Table 2). The area of the resonance at 1.26 ppm was divided by the area of the resonance at 1.39 ppm assigned to CH_2 protons and also was divided by the resonance at 4.1 ppm assigned to the wax ester proton (Fig. 3). By comparing the area of the resonance at 1.26 ppm to the area of two other resonances, we can be assured that the differences observed in Figures 2A and 2C were due to a change in the area of the 1.26-ppm resonance and not to a change in the areas of the 1.39- or 4.1-ppm resonances. The relative area ratios of the 0.94 to 0.84 ppm resonances did not change with MGD (0.17 ± 0.02, 0.18 ± 0.02 for Mn and Md, respectively), nor did the ratio of the area of the 1.03-ppm resonance to the area of the 0.84-ppm resonance change with MGD (0.059 ± 0.005 and 0.051 ± 0.004 for Mn and Md, respectively).

PCA of the CH_2/CH_3 region of NMR Spectra. As further evidence of the relative intensity changes observed in Figure 2, PCA was used to analyze variations within a group of spectra denoted as the training set. PCA finds the variations, in this case the spectral regions, which appear to rise or drop proportionally. These regions are extracted and are referred to as eigenvectors. Eigenvectors are also called loading spectra or factors and, again, they represent components that change their relative contributions from sample to sample. The first step in obtaining eigenvectors from a training set of data is to determine the number of eigenvectors to use. Too many eigenvectors tend to overfit the calibration model, whereas too few eigenvectors result in underfit calibration models and lead to

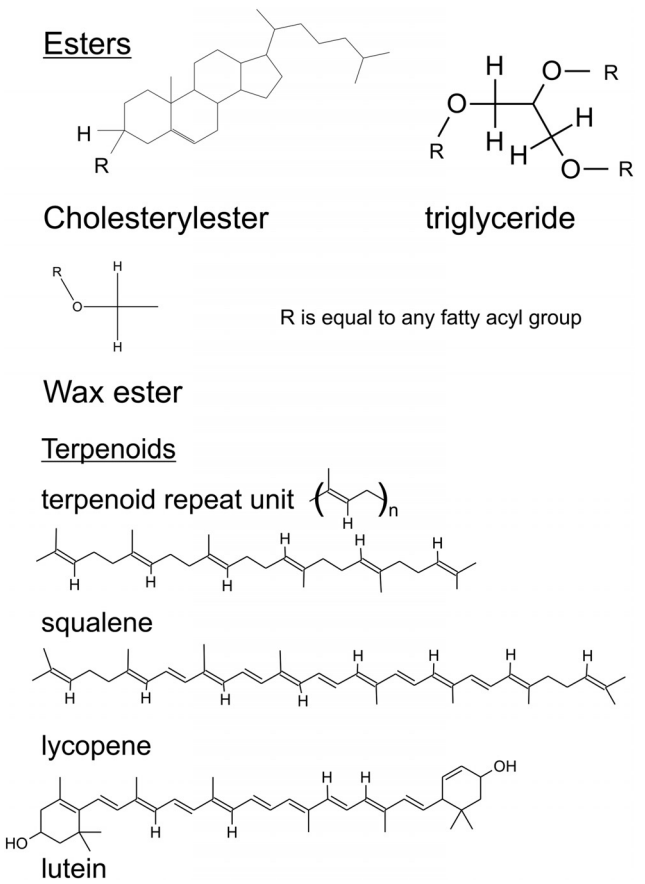

Figure 3. Protons potentially associated with resonances observed in the ^{1}H NMR spectra of human meibum.

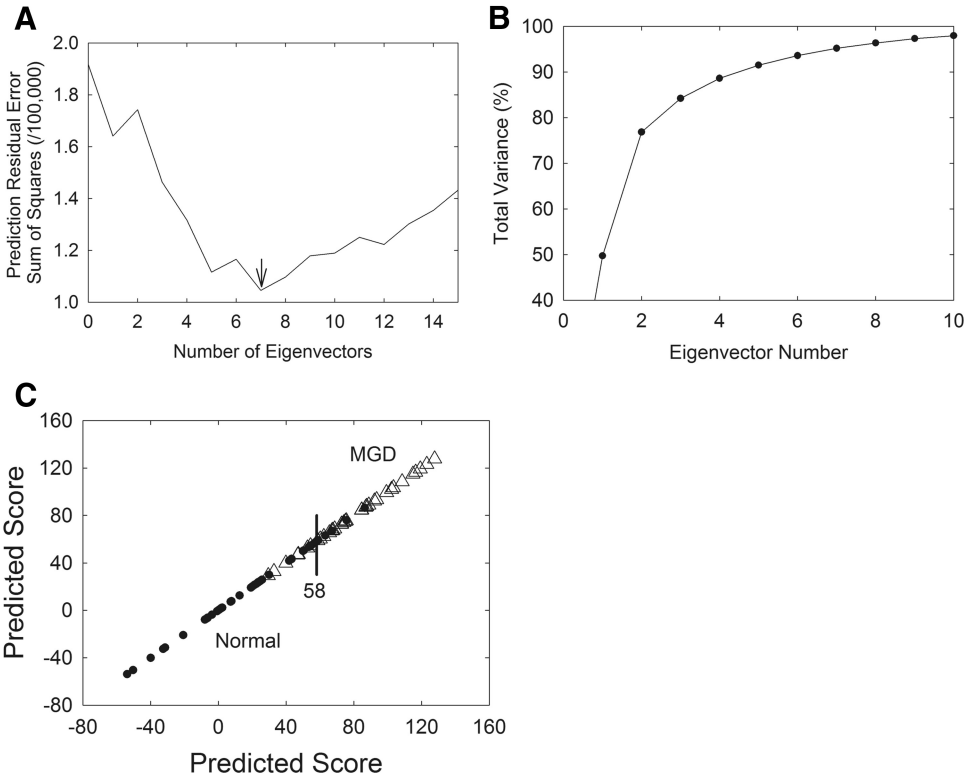

FIGURE 4. (**A**) A PRESS plot was used to choose the proper number of eigenvectors for PCA analysis. The smaller the PRESS value, the better the model is able to predict the contributions of the calibrated constituent MGD/normal scores. (**B**) The contribution of each eigenvector can be evaluated by plotting the eigenvector number versus the percentage of total variance. (**C**) (●) Mn. (△) Md. The training set used in PCA discriminated between Mn and Md, with an accuracy of 86%. A score below 58 was considered normal and above 58 MGD.

inaccurate predictions. To choose the proper number of eigenvectors, we used a prediction residual error sum of the squares (PRESS) plot. The smaller the PRESS value, the better the model is able to predict the contributions of the calibrated constituent MGD/normal scores (Fig. 4A). Seven eigenvectors were necessary to describe most of the variance in our NMR spectra for the constituent MGD/normal score.

The contribution of each eigenvector can be evaluated by plotting the eigenvector number versus the percentage of total variance. In Figure 3B, eigenvectors 1 to 7 accounted for 50%, 27%, 7%, 4%, 3%, 2%, and 2% of the variance in the MGD/normal constituent scores.

Spectral Discrimination. The group of spectra used to generate eigenvectors is called a training set. The training

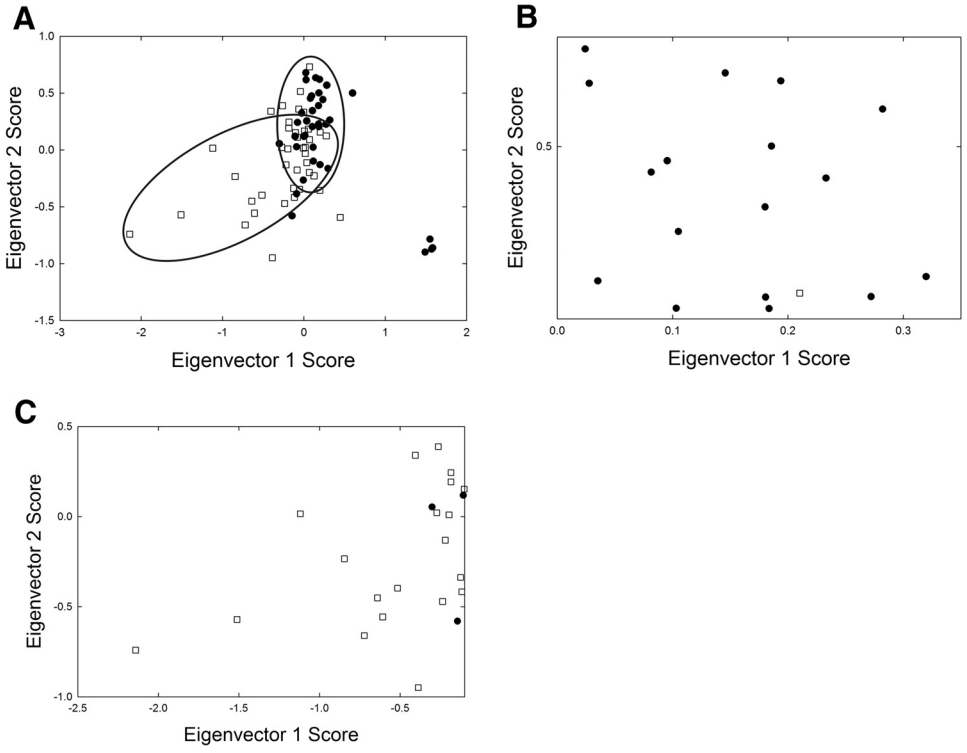

FIGURE 5. The scores for an eigenvector plotted against the scores of another eigenvector were used to determine which eigenvectors were the most important modeling components. (**A**) Eigenvectors 1 and 2 grouped the Mn and Md spectra into two classic elliptical Mahalanobis boundaries. (**B**) A negative score for eigenvectors 1 and 2 favored Mn. (**C**) A positive score favored Md. (●) Md, (□) Mn.

sets may eventually be used to model how the eigenvectors relate to a component, such as age, or in this study, disease. The training set we chose was used to discriminate between Mn and Md, with an accuracy of 86% (Fig. 4C). There was a bias toward more accurately predicting normal samples, 92% compared to predicting MGD samples, 78%. Cross validation was used for each spectrum, removing a spectrum from the training set and using the remaining training set samples to perform the decomposition and calibration calculations. Because we are able to discriminate between Mn and Md, the eigenvectors must contain spectral features that relate to compositional and conformational changes that occur with MGD, as discussed in the following sections.

Scores and Mahalanobis Boundary Groupings. A mathematically reconstructed spectrum can be obtained by adding all the products of each score associated with an eigenvector times the eigenvector. If the PCA model is good, that is if the spectral variations are caused by the principal component (in this case MGD), the reconstructed spectrum will be very similar to the actual original spectrum. The scores for an eigenvector plotted against the scores of another eigenvector were used to determine which eigenvectors were the most important modeling components.

Eigenvectors 1 and 2 grouped the Mn and Md spectra into two classic elliptical Mahalanobis boundaries (Fig. 5A).[61] In general, a negative score for eigenvectors 1 and 2 favored Mn (Fig. 5C) whereas a positive score favored Md (Fig. 5B). Eigen-

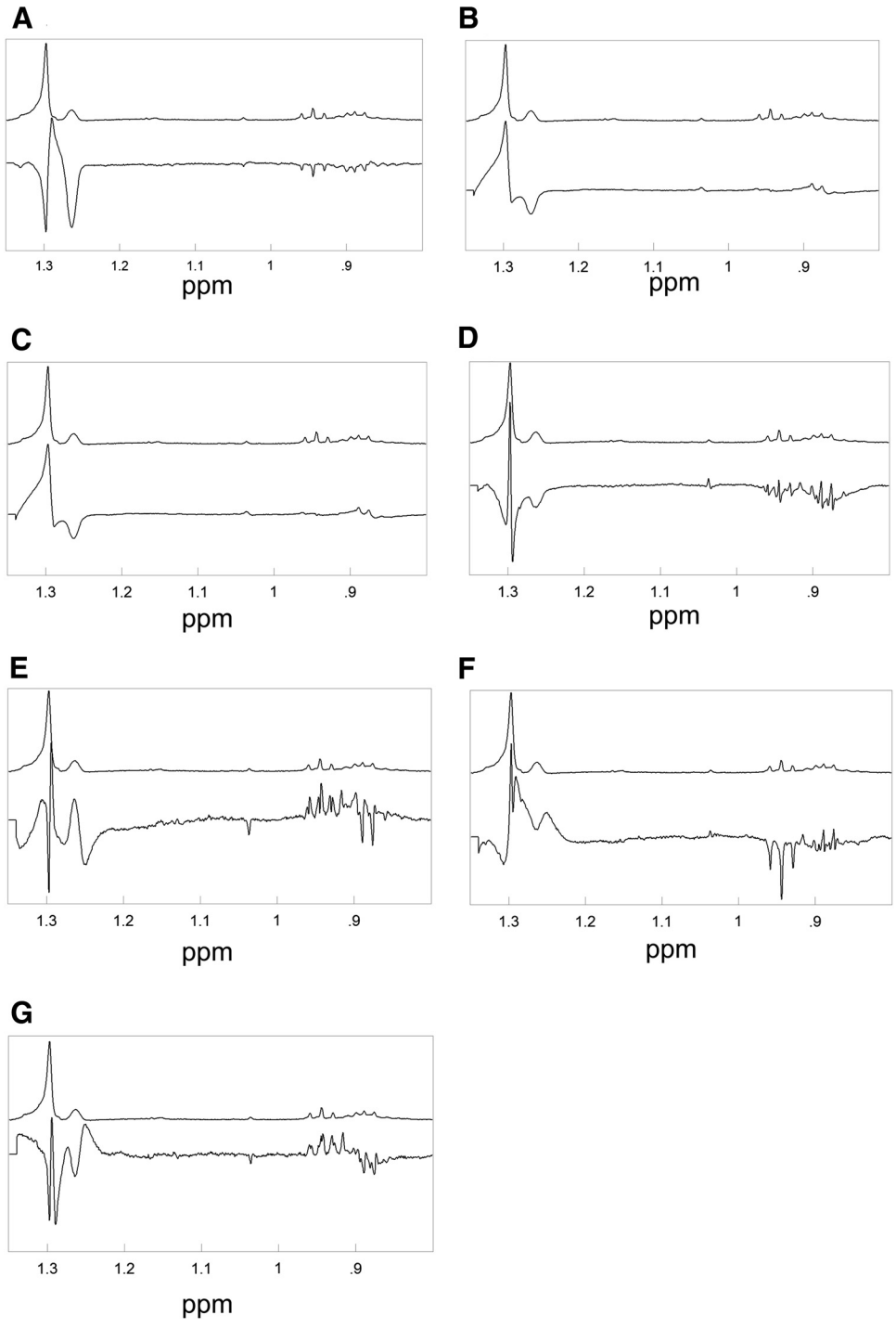

Figure 6. The major eigenvector spectra for the constituent MGD/normal score, used in PCA are shown: (**A**) eigenvector 1, (**B**) eigenvector 2, (**C**) eigenvector 3, (**D**) eigenvector 4, (**E**) eigenvector 5, (**F**) eigenvector 6, (**G**) eigenvector 7. The average spectra of MGD are presented on top in each frame for comparison.

Table 3. Sign of Eigenvector Band Intensity Change

Eigenvector	1.29 ppm	1.26 ppm	0.94 ppm	0.85 ppm
1	−	−	−	−
2	+	−	NC	+
3	−	+	+	−
4	Shift	−	−	−
5	Shift	Shift	−	Shift
6	Shift	Shift	−	Shift
7	Narrow width	Shift	+	Shift

NC, no change.

vectors 1 and 3 grouped the Mn and Md spectra into three classic elliptical Mahalanobis boundaries (data not shown). In general, a positive score for eigenvectors 1 and 3 favored Md (Table 2), whereas a negative score favored Mn (Table 2). The average eigenvector scores for Mn and Md are presented in Table 2. Positive 2 and 3 scores generally favored Md (Fig. 5A), and negative 2 and 3 scores generally favored Mn.

Eigenvector Spectra. The seven major eigenvector spectra for the constituent MGD/normal score, are shown in Figure 6. The eigenvectors 1 to 4 accounted for 88% of the variance in the spectra of Md and Mn (Fig. 4B). Some of the spectral characteristics of the eigenvectors are listed in Table 3.

Positive scores for eigenvectors 1 and 2 favored Md compared with Mn (Fig. 5B). This result means that eigenvectors 1 and 2 were added to the average spectrum to account for the variance of Md. The 1.26-ppm resonance was negative for both eigenvectors 1 and 2 (Table 2) so a lower intensity of the 1.26 resonance of Md was used to discriminate Md from Mn. This finding was confirmed by the relative intensities of the 1.26 ppm resonance (Figs. 2A, 2C).

Eigenvectors 4 through 7 generally account for variability due to shielding and deshielding in the chemical shifts and band width adjustments, rather than intensity differences (Table 3). For example, note in Figure 6E how the eigenvector shows a positive intensity for the 1.26-ppm resonance at higher parts per million and a negative intensity for the 1.26 ppm resonance at slightly lower parts per million. Adding or subtracting this eigenvector would shift the intensity of the 1.26-ppm band.

Double Bond Region

Proton resonances associated with C═C bonds were located between 4.8 and 6 ppm (Fig. 1). One of the most intense proton resonances in the ^{1}H NMR spectra of human meibum appeared at 5.45 ppm and was assigned to *cis* C═C bonds (Fig. 1, Table 4). Three proton resonances associated with other double bonds appeared near 5.2, 5.0, and 4.87 ppm (Fig. 1, Table 4). The resonances near 5 ppm in the ^{1}H NMR spectrum of human meibum have been assigned to squalene by Robosky et al.[49] by comparison of the NMR spectrum of meibum and pure squalene. Others have identified this resonance as the terpenoid squalene in other systems[62–64] and as a general terpenoid in olive oil.[65] As covered in more detail in the Discussion section, it is likely that the bands near 5 are due to the proton (bold underlined) *trans* to the methyl group in the repeating unit: *trans* —$(CH_3C{=}C\underline{\mathbf{H}}CH_2CH_2)_n$— (Fig. 3). This polymer is found in terpenoids in which squalene and the carotenoids lycopene and β carotene are members (Fig. 3). The four resonances due to ═CH protons between 4.8 and 5.5 ppm were lower, but only the area of the 5.2 ppm resonance was significantly lower ($P < 0.05$) for Md compared with Mn from children and adults (Figs. 2B, 2D; Table 5). The relative area of the resonance at 5.2 ppm was measured using the area of the resonances at 1.39 and 4.1, to assure that the differences observed in Figures 2B and 2D were not an anomaly.

Oxidative Products Region

Products of lipid oxidation appear from 5.5 to 10 ppm.[66,67] Four proton resonances were observed at 7.9, 8.7, 9.65, and 9.71 ppm in all the human meibum ^{1}H NMR spectra (Fig. 1; Table 5). The resonances between 6 and 9 ppm were assigned to hydroperoxides and those between 9 and 10 were assigned to aldehydes in accordance with the assignments for oxidized waxes.[66,67]

The sum of the intensity of the resonances in the oxidative products region was significantly lower ($P < 0.05$) for Md

Table 4. Integrated Band Areas Relative to the Area of the 1.39 CH_2 Resonance

Chemical Shifts (ppm)	Normal Child-Adult Unless Indicated	Meibomian Gland Dysfunction	*P*	Tentative Assignment†
0.72	0.00151 ± 0.00022	0.00187 ± 0.00025	0.33	No Assignment
0.89	0.0228 ± 0.0033 (adolescent-adult)	0.026 ± 0.003	0.43	$-C\underline{\mathbf{H}}_3$, except n-3
0.94	0.0043 ± 0.0013	0.0038 ± 0.0004	0.78	$-C\underline{\mathbf{H}}_3$, n-3
1.03	0.0014 ± 0.0002	0.0019 ± 0.0003	0.21	$-CH_2OHCH_2$ $C\underline{\mathbf{H}}_3$ $-CH_2-C\underline{\mathbf{H}}-(CH_3)_2$, isobranched
1.26	0.0041 ± 0.0002	0.0029 ± 0.0002	>0.0001*	$-COO(CH_2)nC\underline{\mathbf{H}}_3$, short chain esters
1.29	0.058 ± 0.009	0.062 ± 0.007	0.72	$-COO(CH_2)nC\underline{\mathbf{H}}_3$, short chain esters
1.39	1	1	1	$-C\underline{\mathbf{H}}_2)_n-$, core,
1.70	0.43 ± 0.043	0.52 ± 0.005	0.17	$R-C\underline{\mathbf{H}}_2-CH_2-COO-R$
4.10	0.026 ± 0.0034	0.025 ± 0.003	0.83	$ROC\underline{\mathbf{H}}_2$-alkyl, wax ester
4.18	0.0031 ± 0.0005	0.003 ± 0.001	1	$CHC\underline{\mathbf{H}}_2OR$; C1, 3 protons, glyceryl. 4 H per molecule
4.25	0.0036 ± 0.0004	0.0033 ± 0.0003	0.55	C1, 3 protons, glyceryl
4.60	0.0047 ± 0.0008	0.0036 ± 0.0007	0.31	$R-O-C\underline{\mathbf{H}}$, C3 of cholesterol ester
4.85	0.014 ± 0.0044 (adolescent-adult)	0.0121 ± 0.0038	0.76	$=C\underline{\mathbf{H}}-$, terpenoid
5.00	0.050 ± 0.097 (adolescent-adult)	0.032 ± 0.0047	0.063	$=C\underline{\mathbf{H}}-$, terpenoid
5.20	0.036 ± 0.0077 (adolescent-adult)	0.0175 ± 0.0029	0.008*	$=C\underline{\mathbf{H}}-$, terpenoid
5.45	0.206 ± 0.013	0.212 ± 0.016	0.79	$-C\underline{\mathbf{H}}=C\underline{\mathbf{H}}-$
7.90	0.0088 ± 0.0013	0.0066 ± 0.0004	0.024*	Hydroperoxides
8.70	0.108 ± 0.012	0.024 ± 0.006	>0.001*	Hydroperoxides
9.65	0.002 ± 0.0008	0.0053 ± 0.0036	0.6	*trans*-2-Alkenals
9.71	0.00026 ± 0.00004	0.00043 ± 0.00007	0.96	$R-C\underline{\mathbf{H}}=O$, *n*-alkenals

* Significantly different, $P < 0.05$.

† The bold underlined proton is the proton for which the tentative assignment was made.

TABLE 5. Relative Band Areas

Chemical Shifts (ppm)	Normal		MGD		Tentative Assignment†
	$A/A_{1.39ppm}$	$A/A_{4.1ppm}$	$A/A_{1.39ppm}$	$A/A_{4.1ppm}$	
0.09	0.0067 ± 0.0046	0.045 ± 0.012	0.00063 ± 0.00008	0.032 ± 0.004	No Assignment
0.72	0.0015 ± 0.0002	0.012 ± 0.03	0.0017 ± 0.0003	0.15 ± 0.03	No Assignment
0.89	0.022 ± 0.003	1.7 ± 0.4	0.025 ± 0.003	1.7 ± 0.2	–C**H**$_3$, except n-3
0.94	0.004 ± 0.001	0.21 ± 0.03	0.0033 ± 0.0003	0.19 ± 0.02	–C**H**$_3$, n-3
1.03	0.0014 ± 0.0002	0.9 ± 0.02	0.0017 ± 0.0003	0.11 ± 0.02	–CH_2OHCH$_2$ C**H**$_3$ –CH_2–C**H**–$(CH_3)_2$, isobranched
1.26	0.0041 ± 0.0002	0.29 ± 0.06*	0.0037 ± 0.0001	0.18 ± 0.02*	–COO(CH_2)nC**H**$_3$, short-chain esters
1.29	0.058 ± 0.009	0.48 ± 0.09	0.054 ± 0.007	0.4 ± 0.1	–COO(CH_2)nC**H**$_3$, short-chain esters
1.39	1	38 ± 4	1	40 ± 5	–(C**H**$_2$)$_n$–, core
1.70	0.43 ± 0.04	36 ± 7	0.52 ± 0.005	45 ± 7	R–C**H**$_2$–CH_2–COO–R
4.10	0.026 ± 0.003	1	0.025 ± 0.003	1	ROC**H**$_2$–alkyl, wax ester
4.18	0.003 ± 0.001	0.20 ± 0.04	0.003 ± 0.001	0.13 ± 0.01	CHC**H**$_2$OR; C1, 3 protons, glyceryl. 4 H per molecule
4.25	0.0036 ± 0.0004	0.25 ± 0.05	0.0033 ± 0.0003	0.27 ± 0.04	C1, 3 protons, glyceryl
4.60	0.0047 ± 0.0008	0.28 ± 0.04*	0.0036 ± 0.0007	0.17 ± 0.02*	R–O–C**H**, C3 of cholesterol ester
5.00	0.042 ± 0.008	3.3 ± 0.8*	0.033 ± 0.005	1.6 ± 0.2*	–C**H**=C**H**–, conjugated
5.20	0.036 ± 0.003	2.7 ± 1.1	0.016 ± 0.005	1.7 ± .7	–C**H**=C**H**–, conjugated
5.45	0.21 ± 0.01	13 ± 2	0.20 ± 0.02	17 ± 2	–C**H**=C**H**–
7.90	0.009 ± 0.001	0.77 ± 0.13	0.0065 ± 0.0005	0.53 ± 0.08	Hydroperoxides
9.65	0.0026 ± 0.0008	0.014 ± 0.002	0.0017 ± 0.006	0.0098 ± 0.0024	*trans*-2-Alkenals
9.71	0.00026 ± 0.00004	0.0037 ± 0.0009	0.00045 ± 0.00009	0.0064 ± 0.0015	R–C**H**=O, *n*-alkenals

* Significantly different, $P < 0.05$.

† The bold underlined proton is the proton for which the tentative assignment was made.

compared with Mn from children and adults (Fig. 7C). This relationship was due to the lower relative intensity of both the 7.85- and 8.6-ppm resonances (Figs. 7A, 7B). As oxidation progresses, the amount of aldehydes increases relative to the amount of hydroperoxides.[66,67] Even though the amounts of hydroperoxides and aldehydes were lower in Md than in Mn (Fig. 7C), the ratio of aldehydes (sum of areas of resonances at 9.65 and 9.71) to hydroperoxides (sum of areas of resonances at 7.9 and 8.7) increased with age and MGD (Fig. 7D). The lower content of hydroperoxides and aldehydes in Md compared with Mn shows the degree of lipid oxidation is less with MGD. Since the ratio of aldehydes to hydroperoxides was larger in Md than in Mn, the breakdown of hydroperoxides was greater in Md (Fig. 7D).

DISCUSSION

When the NMR spectra of Md were compared with those of Mn, three statistically significant decreases were observed in the relative amounts of CH_3 moieties at 1.26 ppm, products of lipid oxidation above 7 ppm, and ═CH moieties at 5.2 ppm

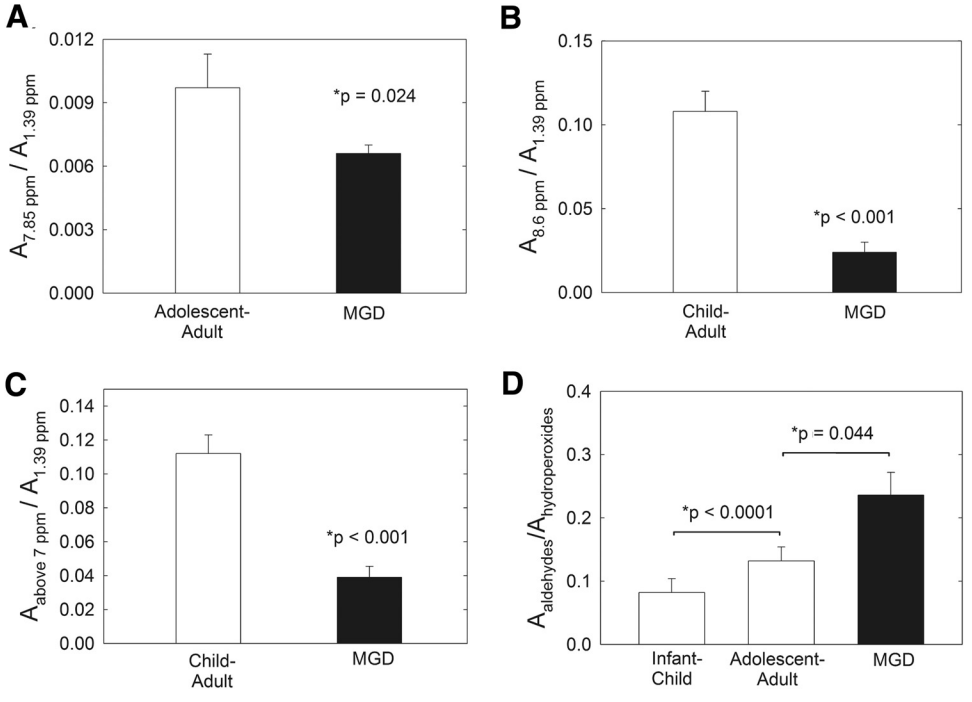

FIGURE 7. (**A**) The ratio $A_{7.85}/A_{1.39}$ is the ratio of hydroperoxides to CH_2 moieties. (**B**) The ratio $A_{8.6}/A_{1.39}$ is the ratio of aldehydes to CH_2 moieties. (**C**) The sum of the area of the resonances in the oxidative products region (resonances >7 ppm) was significantly lower ($P < 0.05$) for Md than for Mn from children and adults. (**D**) The area ratio of aldehydes (sum of the areas of the resonances at 9.65 and 9.71 ppm) to hydroperoxides (sum of the areas of the resonances at 7.9 and 8.7 ppm) increased with age and MGD. As oxidation progressed, the ratio of aldehydes to hydroperoxides generally decreased.

associated with terpenoids. All three changes could account for the higher degree of lipid order of Md compared with age-matched Mn.[37,38] Lipid order was measured as the percentage of *trans* rotomers in the hydrocarbon chains and is related to meibum viscosity.[37,38] The higher the lipid order/viscosity the stronger the lipid–lipid interactions. At 34°C, 47% of the Md hydrocarbons were ordered compared with 35% of the Mn hydrocarbons.[36,37] The major factor governing the order of lipids in the lens[68] and meibum[25,38] is lipid saturation. The decrease in unsaturation in the same samples used in the present study was confirmed by infrared spectroscopy.[22]

Aldehydes and hydroperoxides, which are hydrophilic groups in the hydrophobic hydrocarbon chain region of lipids, inhibit lipid–lipid interactions and fluidize the hydrocarbon chains,[69,70] and therefore the lower level of products of lipid oxidation in Md observed in the present NMR study could also contribute to the higher order of Md compared with Mn.[37,38] Chain length is another factor that is related to lipid order, longer hydrocarbon chains have more extensive van der Waals interactions that contribute to stronger lipid–lipid interactions.[38] A decrease in the shorter chain length segments associated with the 1.26-ppm resonance in the present study would also contribute to lowering the hydrocarbon chain order of Md. In addition to lipid compositional changes that contribute to the ordering of Md hydrocarbon chains, Md has more protein than Mn.[22] The amount of protein and lipid order was related to age in Mn and in MGD.[22]

Lipid order and the amount of lipid observed on the lid margin correlated indirectly. Possibly, and as a consequence of a more ordered viscous meibum with MGD, less lipid flows out of the meibomian gland orifice and, in conjunction with elevated protein content, could facilitate the plugging of the meibomian gland orifices.[71] The amount of lipid on the lid margin with MGD does not influence tear stability, because there is at least 17 times more lipid pooled on the lid margin than is needed to cover the tear surface, even with MGD.[71] However, the lipid composition, especially the lipid in plugged glands, could change. We noted that even though the amount of products of lipid oxidation was lower in Md compared with Mn, the rate of the breakdown of hydroperoxides to aldehydes was higher in Md. Perhaps inflammation and the slower rate of meibum expression contribute to the greater degree of oxidation observed in the present study.

The resonances near 5 ppm in the ^{1}H NMR spectrum of human meibum have been assigned to squalene on the basis of a comparison of the spectra of human meibum versus that of squalene.[49] Others have also identified those resonances to the terpenoid squalene in other systems[62–64,72] and as a general terpenoid in olive oil.[65] A careful NMR evaluation of purified squalene shows that the resonance at 5.1 is from the protons on C3 and C4 carbons, and the resonance at 5.17 ppm is from the proton on C11.[73] In a pilot Raman spectroscopic study, carotenoid-like molecules were found in human meibum.[25] The compounds decreased with increasing age and MGD. In the present study, it is likely that the bands near 5 ppm are due to the proton *trans* to the methyl group in terpenoids (Fig. 3). The repeating unit of the polymer: *trans* —$(CH_3C{=}C\underline{H}CH_2CH_2)_n$— is found in terpenoids in which squalene, and the carotenoids lycopene and β-carotene are members (Fig. 3).

Terpenoids exhibit a plethora of mostly positive biological functions, such as being anticarcinogenic, and possess antimycobacterial properties.[74–76] More than 140,000 papers and more than 8000 review articles have been written on the function of terpenoids to date. The benefits of dietary carotenoids, a type of terpenoid, have been reviewed.[77] Terpenoids protect against many diseases.[78–80] The terpenoid lycopene found in the eye, is a powerful antioxidant[82] that inhibits reactive oxygen production, controls cholesterol synthesis, reduces inflammatory response through changes in cytokine production and regulates apoptosis.[75] Terpenoids are important for biological function and the lower level of terpenes found in Md could influence the composition of meibum, enhanced oxidation, and tear stability.

The terpenoid squalene is a precursor of cholesterol synthesis. It is not surprising that the lower levels of terpenoids found in Md are associated with lower levels of cholesterol esters.[24] Terpenoids influence the fluidity of pure phospholipid vesicals much as cholesterol does, ordering them, lowering their phase transition temperature, and decreasing the cooperativity between the lipids.[83–87] On the other hand, lycopene, a carotenoid, increases the phase transition temperature of microsomes.[88] Therefore, the effect of a decrease in terpenoids on the Md phase transitions would be too speculative to comment on signaling the need for further investigation.

On the surface of the eye, terpenoids could act a surfactants and stabilize the lipid layer, bridging the multiple layers of wax sheets much as they span and reinforce the phospholipid bilayer.[89] Loss of terpenoids with MGD could cause detrimental changes in the structure of the tear film lipid layer. It would be useful to purify and characterize the terpenoids in human meibum to begin to understand their significance.

Future Studies

Future studies will be designed to isolate, identify, and/or confirm the assignment of the resonance at 5.2 ppm. It would also be informative to examine the meibum from donors with other subclasses of MGD. The present study included donors with obvious signs and symptoms of MGD. There are early and mild forms termed nonobvious MGD (NOMGD) that can only be diagnosed by physical expression.[90] Inflammation is not present in NOMGD and is likely to be missed frequently during clinical examination.[90] Spectroscopy could be beneficial as a diagnostic tool if changes in meibum due to NOMGD could be detected, but given the negligible amount of meibum expressed in this variant of MGD, it may be difficult. At present, a standard technique for measuring expressibility is subjective and lacking. A custom expression device, recently developed, could be the solution.[91] In the present study, the meibomian glands were gently but firmly expressed by a single clinician in an effort to obtain uniform results. A custom device that controls the amount of pressure applied to the eye lid could eliminate variability in the quantity and perhaps quality of the meibum obtained from different clinicians or different variants of expression.[91]

In addition to the power of NMR spectroscopy to detect differences in the composition of meibum, NMR is promising as a diagnostic tool. The accuracy of PCA improves with the number of samples. It is reasonable that with more samples PCA of NMR data from human meibum samples could reach an accuracy of 99% or better. The Mahalanobis groupings could be used as a diagnostic tool.

References

1. Brown SI, Dervichian DG. The oils of the meibomian glands: physical and surface characteristics. *Arch Ophthalmol.* 1969;82:537–540.
2. Yokoi N, Takehisa Y, Kinoshita S. Correlation of tear lipid layer interference patterns with the diagnosis and severity of dry eye. *Am J Ophthalmol.* 1996:122;818–824.
3. Hamano H, Hamano T, Hori M, Kawabe H, Mitsunga S. Observations of the precorneal tear film of Sjögren's syndrome by a bio differential interference microscope. *Folia Ophthalmol Jpn.* 1980;31:753–755.

4. Matsumoto Y, Dogru M, Goto E, I et al. Efficacy of a new warm moist air device on tear functions of patients with simple meibomian gland dysfunction. *Cornea.* 2006;25:644–650.
5. Liu DT, Di Pascuale MA, Sawai J, Gao YY, Tseng SC. Tear film dynamics in floppy eyelid syndrome. *Invest Ophthalmol Vis Sci.* 2005;46:1188–1194.
6. Yokoi N, Komuro A. Non-invasive methods of assessing the tear film. *Exp Eye Res.* 2004;78:399–407.
7. Shimazaki J, Sakata M, Tsubota K. Ocular surface changes and discomfort in patients with meibomian gland dysfunction. *Arch Ophthalmol.* 1995;113:1266–1270.
8. Mathers WD. Ocular evaporation in meibomian gland dysfunction and dry eye. *Ophthalmology.* 1993;100:347–351.
9. Craig JP, Blades K, Patel S. Tear lipid layer structure and stability following expression of the meibomian glands. *Ophthalmic Physiol Opt.* 1995;15:569–574.
10. McCulley JP, Sciallis GF. Meibomian keratoconjunctivitis. *Am J Ophthalmol.* 1977;84:788–793.
11. Young G, Efron N. Characteristics of the pre-lens tear film during hydrogel contact lens wear. *Ophthalmic Physiol Opt.* 1991;11:53–58.
12. Korb DR, Greiner JV, Glonek T. Tear film lipid layer formation: Implications for contact lens wear. *Opt Vis Sci.* 1996;73:189–192.
13. Norm MS. Tear break-up time: a review. In: Holly FJ, ed. *The Preocular Tear Film in Health, Disease, and Contact Lens Wear*. Lubbock, TX: Dry Eye Institute;1986:52–55.
14. Foulks GN. The evolving treatment of dry eye. *Ophthalmol Clin North Am.* 2003;16:29–35.
15. Paranjpe DR, Foulks GN. Therapy for meibomian gland disease. *Ophthalmol Clin North Am.* 2003;16:37–42.
16. Bron AJ, Tiffany JM. The meibomian glands and tear film lipids: structure, function, and control. *Adv Exp Med Biol.* 1998;438:281–295.
17. Foulks GN. The correlation between the tear film lipid layer and dry eye disease. *Surv Ophthalmol.* 2007;52:369–374.
18. Green-Church KB, Butovich I, Willcox M, et al. The international workshop on meibomian gland dysfunction: report of the subcommittee on tear film lipids and lipid-protein interactions in health and disease. *Invest Ophthalmol Vis Sci.* 2011;52:1979–1993.
19. Butovich IA, Millar TJ, Ham BM. Understanding and analyzing meibomian lipids: a review. *Curr Eye Res.* 2008;33:405–420.
20. Nicolaides N, Santos EC. The di- and triesters of the lipids of steer and human meibomian glands. *Lipids.* 1985;20:454–467.
21. Borchman D, Foulks GN, Yappert MC. Confirmation of changes in human meibum lipid infrared spectra with age using principal component analysis. *Curr Eye Res.* 2010;35:778–786.
22. Borchman D, Foulks GN, Yappert MC. Changes in human meibum lipid with meibomian gland dysfunction using principal component analysis. *Exp Eye Res.* 2010;91:246–256.
23. Borchman D, Foulks GN, Yappert MC, Milliner SE. Changes in human meibum lipid composition with age using NMR Spectroscopy. *Invest Ophthalmol Vis Sci.* In press.
24. Shrestha RK, Borchman D, Foulks GN, Yappert MC, Milliner SE. Analysis of the composition of lipid in human meibum from normal infants, children, adolescents, adults and adults with meibomian gland dysfunction using ^{1}H-NMR Spectroscopy. *Invest Ophthalmol Vis Sci.* 2011;52:7350–7358.
25. Oshima Y, Sato H, Zaghloul A, Foulks GN, Yappert MC, Borchman D. Characterization of human meibum lipid using Raman spectroscopy. *Curr Eye Res.* 2009;34:824–835.
26. Shine WE, McCulley JP. The role of cholesterol in chronic blepharitis. *Invest Ophthalmol Vis Sci.* 1991;32:2272–2280.
27. Shine WE, McCulley JP. Meibomian gland triglyceride fatty acid differences in chronic blepharitis patients. *Cornea.* 1996;15:340–346.
28. Shine WE, McCulley JP. Association of meibum oleic acid with meibomian seborrhea. *Cornea.* 2000;19:72–74.
29. Joffre C, Souchier M, Leclere L, et al. Branched-chain fatty acids, increased in tears of blepharitis patients, are not toxic for conjunctival cells. *Br J Ophthalmol.* 2009;93:1391–1395.
30. Shine WE, McCulley JP. Keratoconjunctivitis sicca associated with meibomian secretion polar lipid abnormality. *Arch Ophthalmol.* 1998;116:849–852.
31. Shine WE, McCulley JP. Meibomianitis: polar lipid abnormalities. *Cornea.* 2004;23:781–783.
32. Butovich IA, Uchiyama E, Di Pascuale MA, et al. Liquid chromatography-mass spectrometric analysis of lipids present in human meibomian gland secretions. *Lipids.* 2007;42:765–776.
33. Butovich IA, Uchiyama E, McCulley JP. Lipids of human meibum: mass-spectrometric analysis and structural elucidation. *J Lipid Res.* 2007;48:2220–2235.
34. Butovich IA. On the lipid composition of human meibum and tears: comparative analysis of nonpolar lipids. *Invest Ophthalmol Vis Sci.* 2008;49:3779–3789.
35. Butovich IA, Wojtowicz JC, Molai M. Human tear film and meibum: very long chain wax esters and (O-acyl)-omega-hydroxy fatty acids of meibum. *J Lipid Res.* 2009;50:2471–2485.
36. Butovich IA. Cholesteryl esters as a depot for very long chain fatty acids in human meibum. *J Lipid Res.* 2009;50:501–513.
37. Foulks GN, Borchman D, Yappert MC, Kim S, McKay JW. Topical azithromycin therapy of meibomian gland dysfunction: clinical response and lipid alterations. *Cornea.* 2010;29:781–788.
38. Borchman D, Foulks GN, Yappert MC, et al. Human meibum lipid conformation and thermodynamic changes with meibomian-gland dysfunction. *Invest Ophthalmol Vis Sci.* 2011;52:3805–3817.
39. Foulks GN, Borchman D. Meibomian gland dysfunction: the past, the present, the future. *Eye Contact Lens.* 2010;36:249–253.
40. Borchman D, Foulks GN, Yappert MC, et al. Physical changes in human meibum with age as measured by infrared spectroscopy. *Ophthalmic Res.* 2010;44:34–42.
41. Borchman D, Foulks GN, Yappert MC, Tang D, Ho DV. Spectroscopic evaluation of human tear lipids. *Chem Phys Lipids.* 2007;147:87–102.
42. Borchman D, Foulks GN, Yappert MC, Ho DV. Temperature-induced conformational changes in human tear lipids hydrocarbon chains. *Biopolymers..* 2007;87:124–133.
43. Huang L, Grami V, Marrero Y, et al. Human lens phospholipid changes with age and cataract. *Invest Ophthalmol Vis Sci.* 2005;46:1682–1689.
44. Estrada R, Puppato A, Borchman D, Yappert MC. Re-evaluation of the phospholipid composition in membranes of adult human lenses by ^{31}P NMR and MALDI-MS. *Biochim Biophys Acta.* 2010;1798:303–311.
45. Ferguson-Yankey S, Borchman D, Taylor KG, DuPre DB, Yappert MC. Conformational Studies of sphingolipids by NMR spectroscopy, I: dihydrosphingomyelin. *Biochim Biophys Acta.* 2000;1467:307–325.
46. Borchman D, Byrdwell WC, Yappert MC. Regional and age-dependent differences in the phospholipid composition of human lens membranes. *Invest Ophthalmol Vis Sci.* 1994;35:3938–3942.
47. Byrdwell WC, Borchman D, Porter RA, Taylor KG, Yappert MC. Separation and characterization of the unknown phospholipid in human lens membranes. *Invest Ophthalmol Vis Sci.* 1994;35:4333–4343.
48. Merchant TE, Lass JH, Meneses P, Greiner JV, Glonek T. Human crystalline lens phospholipid analysis with age. *Invest Ophthalmol Vis Sci.* 1991;32:549–555.
49. Robosky LC, Wade K, Woolson D, et al. Quantitative evaluation of sebum lipid components with nuclear magnetic resonance. *J Lipid Res.* 2008;49:686–692.
50. Tulloch AP. Solvent effects on the nuclear magnetic resonance spectra of methyl hydroxysterates. *J Am Oil Chem Soc.* 1966;43:670–674.
51. Verardo G, Pagani E, Geatti P. A thorough study of the surface wax of apple fruits. *Anal Biochem.* 2003;376:659–667.
52. Frost DJ, Barzilay J. Proton magnetic resonance identification of nonconjugated cis-unsatureated fatty acids and esters. *Anal Chem.* 1971;43:1316–1318.
53. Scano P, Marincola FC, Locci E, Lai A. ^{1}H and ^{13}C NMR studies of melon and head blubber of the striped dolphin (Stenella coeruleoalba). *Lipids.* 2006;41:1039–1048.

54. Tulloch AP. Beeswax: structure of the esters and their component hydroxyl acids and diols. *Chem Phys Lipids.* 1971;6:235–265.
55. Wineburg JP, Swern D. NMR chemical shift reagents in structural determination of lipid derivatives, II: methyl petroselinate and methyl oleate. *J Am Oil Chem Soc.* 1971;49:267–273.
56. KE PJ, Ackman RG. NMR determination of wax esters in marine lipids. *Anal Chem Acta.* 1974;69:253–258.
57. Purcell JM, Morris SG, Susi H. Proton magnetic resonance spectra of unsaturated fatty acids. *Anal Chem.* 1966;38:588–592.
58. Johnson LF, Shoolery JN. Determination of unsaturation and average molecular weight of natural fats by nuclear magnetic resonance. *Anal Chem.* 1962;34:1136–1139.
59. Glass CA, Dutton HJ. Determination of beta-olefinic methyl groups in esters of fatty acids by nuclear magnetic resonance. *Anal Chem.* 1964;36:2401–2404.
60. Foulks GN, Bron AJ. Meibomian-gland dysfunction: a clinical scheme for description, diagnosis, classification and grading. *Ocul Surf.* 2003;1:17–36.
61. Mahalanobis PC. On the generalized distance in statistics. *Proc Natl Inst Sci India.* 1936;2:49–55.
62. Achitouv E, Metzer P, Marie-Noëlle R, Largeau C. C_{31}-C_{34} methylated squalenes from a Bolivian strain of Botryococcus braunii. *Phytochemistry.* 2004;65:3159–3165.
63. Corcelli A, Lattanzio VMT, Mascolo G, Papadia P, Fanizzi F. Lipid-protein stoichiometries in a crystalline biological membrane: NMR quantitative analysis of the lipid extract of the purple membrane. *J Lipid Res.* 2002;43:132–140.
64. Quang DN, Hashimoto T, Tanaka M, et al. Concentoils B, C and D, three squalene-type triterpenoids from the ascomycete Daldinia concentrica. *Phytochemistry.* 2002;61:345–353.
65. D'Imperio M, Gobbing M, Picanza A, Costanzo S, Della Corte A, Mannina L. Influence of harvest method and period on olive oil composition: an NMR and statistical study. *J Agric Food Chem.* 2010;58:11043–11051.
66. Haywood RM, Claxson AW, Hawkes GE, et al. Detection of aldehydes and their conjugated hydroperoxydiene precursors in thermally-stressed culinary oils and fats: investigations using high resolution proton NMR spectroscopy. *Free Radic Res.* 1995;22:441–482.
67. Guillén MD, Ruiz A. Oxidation process of oils with high content of linoleic acyl groups and formation of toxic hydroperoxy- and hydroxyalkenals: a study by ^{1}H nuclear magnetic resonance. *J Sci Food Agric.* 2005;85:2413–2420.
68. Borchman D, Yappert MC. Lipids and the Ocular Lens. *J Lipid Res.* 2010;51:2473–2488.
69. Lamba OP, Lal S, Yappert MC, Borchman D. Spectroscopic detection of lipid peroxidation products and structural changes in a sphingomyelin model system. *Biochem Biophys Acta.* 1991;1081:181–187.
70. Lamba OP, Borchman D, Garner WH. Spectral characterization of lipid peroxidation in rabbit lens membranes induced by hydrogen peroxide in the presence of Fe^{2+}/Fe^{3+}: A site-specific catalyzed oxidation. *Free Rad Biol Med.* 1994;16:591–601.
71. Ashraf Z, Pasha U, Greenstone V, et al. Quantification of human sebum on skin and human meibum on the eye lid margin using sebum tape, spectroscopy and chemical analysis. *Curr Eye Res.* 2011;36:553–562.
72. Huang Z, Poulter CD. Tetramethylsqualene, a triterpene from Botryococcus braunii var. show A. *Phytochemistry.* 1989;28:1467–1470.
73. Pogliani L, Ceruti M, Ricchiardi G, Viterbo D. An NMR and molecular mechanics study of squalene and squalene derivatives. *Chem Phys Lipids.* 1994;70:21–34.
74. Huang MT, Ho CT, Wang ZY, et al. Inhibition of skin tumorigenesis by rosemary and its constituents carnosol and ursolic acid. *Cancer Res.* 1994;54:701–708.
75. Palozza P, Parrone N, Simone RE, Catalano A. Lycopene in atherosclerosis prevention: an integrated scheme of the potential mechanisms of action from cell culture studies. *Arch Biochem Biophys.* 2010;504:26–33.
76. Noro J, Barrows LR, Gideon J, et al. Tetrahydroxysqualene from *Rhus taitensis* shows antimycobacterial activity against *Mycobacterium tuberculosis*. *J Nat Prod*. 2008;71:1623–1624.
77. Namitha KK, Megi PS. Chemistry and biotechnology of carotenoids. *Crit Rev Food Sci Nutr.* 2010;50:728–760.
78. N.I. Krinsky. The biological properties of carotenoids. *Pure Appl Chem.* 1994;66:1003–1010.
79. JL Schwartz. In vitro biological methods for determination of carotenoid activity. *Methods Enzymol.* 1993;214:226–256.
80. Mayne ST. Beta-carotene, carotenoids, and disease prevention in humans. *FASEB J.* 1996;10:690–701.
81. Bara A, Socaciu C, Neamtu G. Effects of some carotenoids on proliferation and nucleotide turnover in Ehrlich ascites. *Radioter Oncol Med.* 1995;2:16–21.
82. DiMascio P, Kaiser S, Sies H. Lycopene as the most efficient biological carotenoid singlet oxygen quencher. *Arch Biochem Biophys.* 1989;274:532–538.
83. Mishra NN, Liu GY, Yeaman MR, et al. Carotenoid-related alteration of cell membrane fluidity impacts Staphylococcus aureus susceptibility to host defense peptides. *Antimicrob Agents Chemother.* 2011;55:526–531.
84. Subczynski WK, Markowska E, Gruszecki WI, Sielewiesiuk J. Effects of polar carotenoids on dimyristoylphosphatidylcholine membranes: a spin-label study. *Biochim Biophys Acta.* 1992;1105:97–108.
85. Strzałka K, Gruszecki WI. Effect of beta-carotene on structural and dynamic properties of model phosphatidylcholine membranes, I: an EPR spin label study. *Biochim Biophys Acta.* 1994;1194:138–142.
86. Socaciu C, Jessel R, Diehl HA. Competitive carotenoid and cholesterol incorporation into liposomes: effects on membrane phase transition, fluidity, polarity and anisotropy. *Chem Phys Lipids.* 2000;106:79–88.
87. Wisniewska A, Widomska J, Subczynski WK. Carotenoid-membrane interactions in liposomes: effect of dipolar, monopolar, and nonpolar carotenoids. *Acta Biochim Pol.* 2006;53:475–484.
88. Socaciu C, Jessel R, Diehl HA. Carotenoid incorporation into microsomes: yields, stability and membrane dynamics. *Spectrochim Acta A Mol Biomol Spectrosc.* 2000;56:2799–2809.
89. Rohmer M, Bouvier P, Ourisson G. Molecular evolution of biomembranes: structural equivalents and phylogenetic precursors of sterols. *Proc Natl Acad Sci U S A.* 1979;76:847–851.
90. Blackie CA, Korb DR, Knop E, Bedi R, Knop N, Holland EJ. Nonobvious obstructive meibomian gland dysfunction. *Cornea.* 2010;29:1333–1345.
91. Korb DR, Blackie CA. Meibomian gland diagnostic expressibility: correlation with dry eye symptoms and gland location. *Cornea.* 2008;27:1142–1147.